

Gas-Phase Electron Diffraction Studies on Two 11-Vertex Dicarboranes, *closo*-2,3-C₂B₉H₁₁ and *nido*-2,9-C₂B₉H₁₃Iain D. Mackie,[†] Heather E. Robertson,[†] David W. H. Rankin,^{*†} Mark A. Fox,[‡] and John M. Malget[‡]*School of Chemistry, University of Edinburgh, West Mains Road, Edinburgh EH9 3JJ, U.K., and Chemistry Department, Durham University Science Laboratories, South Road, Durham DH1 3LE, U.K.*

Received April 29, 2004

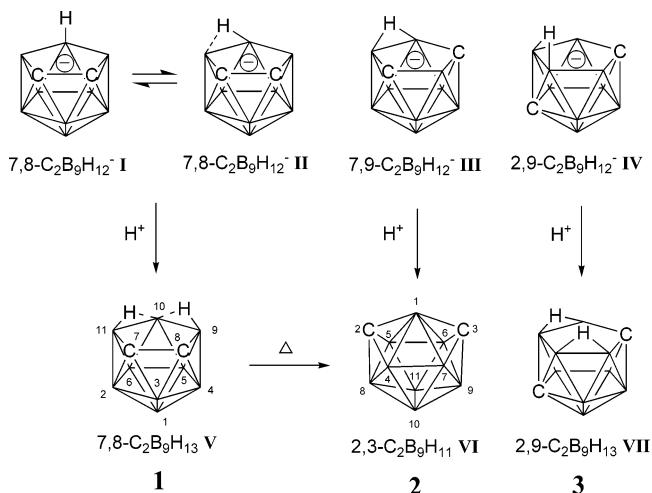
The molecular structures of two carboranes, *closo*-2,3-C₂B₉H₁₁ and *nido*-2,9-C₂B₉H₁₃, were determined experimentally for the first time using gas-phase electron diffraction (GED). For *closo*-2,3-C₂B₉H₁₁, a model with C_{2v} symmetry was refined to give C–B bond distances ranging 158.3–167.0 pm and B–B distances ranging 177.4–200.0 pm. The structure of *nido*-2,9-C₂B₉H₁₃ was refined using a model with C_s symmetry to give C–B bond lengths ranging 160.3–171.9 pm and B–B lengths ranging 173.0–196.1 pm. Ab initio computations (up to MP2/6-311+G*) were also carried out on these and the related *nido*-7,8-C₂B₉H₁₃, which was not sufficiently stable to allow determination of its molecular structure by GED.

Introduction

Since the pioneering work of Hawthorne and co-workers in the 1960s,^{1,2} the 11-vertex dicarboranes and derivatives have been widely used as precursors to a vast number of metallocarboranes.^{3–5} These carboranes are also common precursors to a large number of heteroboranes, an area exploited mainly by the Czech groups of Plešek and Štíbr.⁶ However, the structures of the neutral 11-vertex dicarboranes C₂B₉H₁₁ and C₂B₉H₁₃ and their anions C₂B₉H₁₂[−] have only recently been investigated.

In 1992, the first structural report on a parent 11-vertex dicarborane concerned an X-ray study by Welch et al. on anion 7,8-C₂B₉H₁₂[−] as the (Me₂SO)₂H⁺ salt.⁷ This study revealed a symmetrical endo-hydrogen on the open face

Scheme 1



Each naked vertex represents BH

Each C vertex contains one exo H

(geometry **I** in Scheme 1). At Durham, two salts of anion 7,8-C₂B₉H₁₂[−] were also structurally characterized by X-ray crystallography.^{8,9} The anion in each salt was found to contain an unsymmetrical endo-hydrogen on the open face (geometry **II** in Scheme 1). Salts of the related anions 7,9-

* Author to whom correspondence should be addressed. E-mail: d.w.h.rankin@ed.ac.uk.

[†] University of Edinburgh.

[‡] Durham University Science Laboratories.

- (1) (a) Hawthorne, M. F.; Young, D. C.; Andrews, T. D.; Howe, D. V.; Pilling, R. L.; Pitts, A. D.; Reintjes, M.; Warren, L. F.; Wegner, P. A. *J. Am. Chem. Soc.* **1968**, *90*, 879. (b) Wiesboeck, R. A.; Hawthorne, M. F. *J. Am. Chem. Soc.* **1964**, *86*, 1642. (c) Tebbe, F. N.; Garrett, P. M.; Hawthorne, M. F. *J. Am. Chem. Soc.* **1968**, *90*, 869.
- (2) Tebbe, F. N.; Garrett, P. M.; Hawthorne, M. F. *J. Am. Chem. Soc.* **1964**, *86*, 4222.
- (3) Busby, D. C.; Hawthorne, M. F. *Inorg. Chem.* **1982**, *21*, 4101.
- (4) Greenwood, N. N.; Earnshaw, A. *Chemistry of the Elements*, 1st ed.; Pergamon Press: Oxford, 1984; p 209.
- (5) (a) Grimes, R. N. *Coord. Chem. Rev.* **2000**, *200*, 773. (b) Grimes, R. N. In *Comprehensive Organometallic Chemistry II*; Abel, E. W., Stone, F. G. A., Wilkinson, G., Eds.; Pergamon Press: Oxford, 1995; Vol. 1, Chapter 9. (c) Hawthorne, M. F. *Acc. Chem. Res.* **1968**, *1*, 281. (d) Saxena, A. K.; Hosmane, N. S. *Chem. Rev.* **1993**, *93*, 1081.
- (6) (a) Plešek, J.; Heřmánek, S. *Inorg. Synth.* **1984**, *22*, 231. (b) Štíbr, B. *Chem. Rev.* **1992**, *92*, 225.

(7) Buchanan, J.; Hamilton, E. J. M.; Reed, D.; Welch, A. J. *J. Chem. Soc., Dalton Trans.* **1990**, 677.

(8) Davidson, M. G.; Fox, M. A.; Hibbert, T. G.; Howard, J. A. K.; Mackinnon, A.; Neretin, I. S.; Wade, K. *Chem. Commun.* **1999**, 1649.

(9) Fox, M. A.; Goeta, A. E.; Howard, J. A. K.; Hughes, A. K.; Johnson, A. L.; Keen, D. A.; Wade, K.; Wilson, C. C. *Inorg. Chem.* **2001**, *40*, 173.

and 2,9-C₂B₉H₁₂⁻ have also been structurally characterized at Durham with geometries **III** and **IV** (Scheme 1), respectively.¹⁰ There have been many other crystallographic studies of 7,8-C₂B₉H₁₂⁻, and a few of 7,9-C₂B₉H₁₂⁻, but in none of these has the position of the endo-hydrogen been located accurately. All of the three neutral carbaboranes, 7,8-C₂B₉H₁₃ (**1**), 2,3-C₂B₉H₁₁ (**2**), and 2,9-C₂B₉H₁₃ (**3**), were synthesized by acidification with concentrated sulfuric acid of the three monoanions, 7,8-, 7,9-, and 2,9-C₂B₉H₁₂⁻, respectively (see Scheme 1).^{10,11} Molecular geometries of sublimable solids **1–3** were proposed on the basis of NMR data to be of forms **V**, **VI**, and **VII** (Scheme 1), respectively.^{12–14} The existence of these geometries in solution was supported in solution by ab initio/NMR computations.^{10,11}

Of the three neutral dicarbaboranes **1–3**, only two derivatives were structurally characterized. Both were derivatives of **2**, the dimethyl derivative, 2,3-Me₂-2,3-C₂B₉H₉ (**4**), and the pentasubstituted derivative, 10-Br-4,7-(OH)₂-2,3-Me₂-2,3-C₂B₉H₉ (**5**).^{15,16} Structural data for dimethyl derivative **4** determined by X-ray crystallography back in 1966, however, contain only bond distances.¹⁵ The X-ray data on bromo compound **5** revealed a nido-like cage geometry (similar to **III**, Scheme 1) rather than the expected closed-cage geometry **VI**.¹⁶ Compound **2** is the only one of the well-known closo-dicarbaboranes of formula C₂B_nH_{n+2} to contain an unfavorable 7-coordinate boron.

Because we have not been successful in Durham in obtaining suitable crystals of **1–3** for X-ray crystallography, we report here the results of the gas-phase electron diffraction (GED) studies carried out on all of the three neutral carbaboranes at Edinburgh.

Results and Discussion

Gas-Phase Electron Diffraction. Of the three neutral 11-vertex dicarbaboranes **1–3**, we succeeded in determining the molecular structures by GED for closo-carbaborane **2** and carbons-apart nido-carbaborane **3**. Compound **1** proved unsuitable for GED, because not enough vapor pressure could be generated to allow acceptable data to be collected. At higher temperatures, which would generate the required vapor pressure for GED, it decomposed to 2,3-C₂B₉H₁₁ (**2**).²

The model used for the GED refinement of **2** was based upon the optimized geometry obtained by ab initio calculations. The least-squares refinement of the structure resulted in an *R*_G factor of 0.041, with the resultant parameter values listed in Table 1, where they are compared with the results of the highest level ab initio calculations. Parameters obtained at all levels of calculations are listed in Supporting Informa-

Table 1. Geometrical Parameters (*r*_{hl} Structure) for **2**^{a,b}

	parameter	GED	MP2/6-311+G*
<i>p</i> ₁	<i>r</i> B _m ^c	182.8(3)	180.1
<i>p</i> ₂	<i>d</i> 1 ^c	-5.9(5)	-6.2
<i>p</i> ₃	<i>d</i> 2 ^c	-0.4(1)	-0.4
<i>p</i> ₄	∠B(8)	16.9(4)	14.7
<i>p</i> ₅	roB(1) ^c	271.2(5)	270.9
<i>p</i> ₆	roC(2) ^c	259.6(11)	254.1
<i>p</i> ₇	∠C(2)	35.3(3)	39.3
<i>p</i> ₈	∠BBB	103.1(2)	103.9
<i>p</i> ₉	BBBB	-32.7(2)	-32.8
<i>p</i> ₁₀	<i>r</i> H _m ^c	117.2(3)	115.4
<i>p</i> ₁₁	<i>d</i> 3 ^c	11.4(4)	10.6
<i>p</i> ₁₂	<i>d</i> 4 ^c	0.3(1)	0.3
<i>p</i> ₁₃	∠HBB1	161.2(1)	161.2
<i>p</i> ₁₄	φHBBB1	180.0(2)	180.0
<i>p</i> ₁₅	∠HCB	128.2(2)	128.2
<i>p</i> ₁₆	φHCBB	180.0(2)	180.0
<i>p</i> ₁₇	∠HBB2	114.6(2)	114.6
<i>p</i> ₁₈	φHBBB2	165.6(2)	165.7
<i>p</i> ₁₉	∠HBC	120.4(2)	120.4
<i>p</i> ₂₀	φHBCB	180.0(2)	180.0
<i>p</i> ₂₁	∠HBB3	127.6(2)	127.6
<i>p</i> ₂₂	φHBBB3	180.0(2)	180.0

^a Distances in pm; angles in deg. ^b Parameters are defined fully in the Experimental Section. ^c m = mean; *d* = difference; o represents the origin.

Table 2. Selected Bond Distances (*r*_{hl}/pm) and Amplitudes of Vibration (*u*/pm) Obtained in the GED Refinement of the Structure of **2**

<i>u</i>	atom pair	<i>r</i> _{hl}	amplitude	MP2/6-311+G*
<i>u</i> ₁	B(1)–C(2)	162.2(11)	6.8 (tied to <i>u</i> ₅)	163.1
<i>u</i> ₃	B(1)–H(22)	121.0(3)	8.1 (fixed)	119.0
<i>u</i> ₅	C(2)–B(5)	157.9(5)	7.2(1)	157.9
<i>u</i> ₆	C(2)–B(8)	167.0(11)	6.8 (tied to <i>u</i> ₅)	166.8
<i>u</i> ₇	C(2)–H(17)	109.6(4)	7.3 (fixed)	108.4
<i>u</i> ₁₂	B(4)–B(7)	188.6(11)	13.5(5)	187.0
<i>u</i> ₁₄	B(4)–B(10)	180.7(3)	7.0 (tied to <i>u</i> ₂₃)	177.9
<i>u</i> ₁₅	B(4)–H(16)	120.7(3)	8.1 (fixed)	118.7
<i>u</i> ₂₃	B(7)–B(9)	177.4(6)	6.7(2)	180.1
<i>u</i> ₂₆	B(8)–B(10)	180.8(3)	7.9 (tied to <i>u</i> ₂₃)	178.3
<i>u</i> ₂₈	B(8)–H(13)	120.7(3)	8.1 (fixed)	118.7
<i>u</i> ₃₂	B(10)–B(11)	186.6(5)	7.4 (tied to <i>u</i> ₁₂)	184.1
<i>u</i> ₃₃	B(10)–H(12)	121.0(3)	8.1 (fixed)	119.0
<i>u</i> ₃₅	B(1)–B(4)	200.0(7)	24.6(9)	206.7

tion Table S1. Of the 22 geometrical parameters, 8 refined without the application of restraints; the restraints, applied using the SARACEN method,¹⁷ are given in Supporting Information Table S2. A summary of final bond distances and amplitudes of vibration is given in Table 2, and the full list is in Supporting Information Table S3. The least-squares correlation matrix for the structural refinement is given in Supporting Information Table S4. The molecular scattering curves (Supporting Information Figure S1) and the radial distribution curve (Figure 1) show the quality of the fit of the experimental data. Figure 2 shows the molecular structure of **2** determined by GED with the numbering scheme used for the cage atoms.

The geometry obtained in the ab initio optimizations (Supporting Information Table S5) was used as the basis of the model for GED refinement of **3**, which resulted in an

(10) Fox, M. A.; Goeta, A. E.; Hughes, A. K.; Johnson, A. L. *J. Chem. Soc., Dalton Trans.* **2002**, 2132.

(11) Fox, M. A.; Hughes, A. K.; Malget, J. M. *J. Chem. Soc., Dalton Trans.* **2002**, 3505.

(12) Fontaine, X. L. R.; Greenwood, N. N.; Kennedy, J. D.; Nestor, K.; Thornton-Pett, M.; Heřmánek, S.; Jelínek, T.; Štíbr, B. *J. Chem. Soc., Dalton Trans.* **1990**, 681.

(13) Tebbe, F. N.; Garrett, P. M.; Hawthorne, M. F. *J. Am. Chem. Soc.* **1968**, *90*, 869.

(14) Plešek, J.; Heřmánek, S. *Chem. Ind. (London)* **1973**, 381.

(15) Tsai, C.-C.; Streib, W. E. *J. Am. Chem. Soc.* **1966**, *88*, 4513.

(16) Leonowicz, M. E.; Scholer, F. R. *Inorg. Chem.* **1980**, *19*, 122.

(17) (a) Blake, A. J.; Brain, P. T.; McNab, H.; Miller, J.; Morrison, C. A.; Parsons, S.; Rankin, D. W. H.; Robertson, H. E.; Smart, B. A. *J. Chem. Phys.* **1996**, *100*, 12280. (b) Brain, P. T.; Morrison, C. A.; Parsons, S.; Rankin, D. W. H. *J. Chem. Soc., Dalton Trans.* **1996**, 4589. (c) Mitzel, N. W.; Rankin, D. W. H. *J. Chem. Soc., Dalton Trans.* **2003**, 3650.

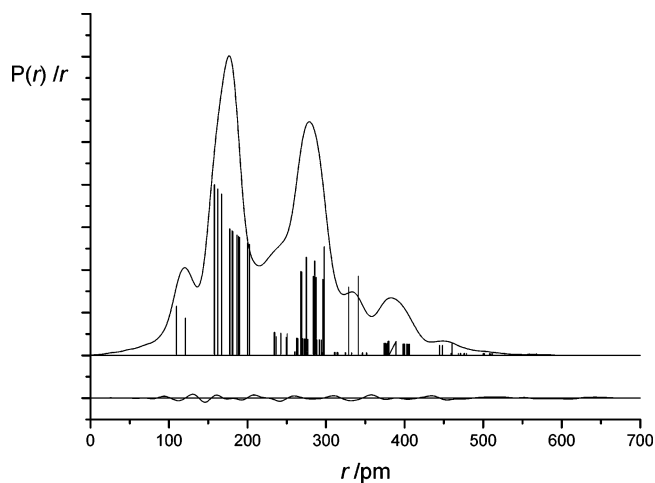


Figure 1. Experimental and difference (experimental – theoretical) radial distribution curves, $P(r)/r$, for **2**. Before Fourier inversion, the data were multiplied by $s \cdot \exp(-0.00002s^2)/(Z_B - f_B)/(Z_C - f_C)$.

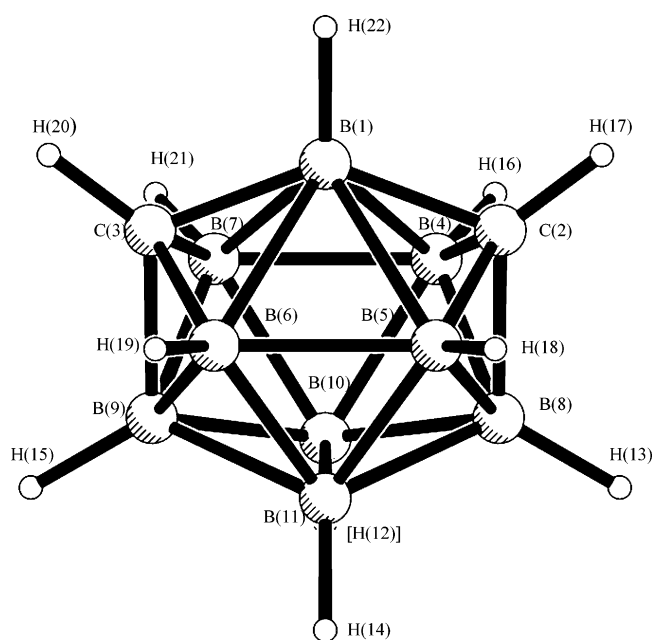


Figure 2. Molecular framework for **2**.

R_G factor of 0.035. The geometrical parameter values are listed in Table 3, and the most significant bond distances and amplitudes of vibration are recorded in Table 4, with the full list in Supporting Information Table S6. Of the 25 parameters, 5 refined freely, and restraints were applied to the remainder, as detailed in Supporting Information Table S7. The least-squares correlation matrix for the structural refinement is presented in Supporting Information Table S8. The radial distribution curve (Figure 3) and the molecular scattering curves (Supporting Information Figure S2) show how well the experimental data fit the refined model structure, which is shown in Figure 4.

Ab Initio Calculations. From examination of the optimized geometries of **2** and **3** at Hartree–Fock (HF), B3LYP, and Moeller–Plesset second-order (MP2) levels of theory, the cage distances show some signs of sensitivity to increased levels of theory. In particular, HF methods generally overestimate the B–B and C–B bond distances and under-

Table 3. Geometrical Parameters (r_{h1} Structure) for **3**^{a,b}

parameter	GED	MP2/6-311+G*	
p_1	r_m	181.2(2)	178.2
p_2	$d1^c$	17.5(1)	17.5
p_3	$d2^c$	15.9(1)	16.0
p_4	$d3^c$	20.7(1)	20.8
p_5	$d4^c$	8.5(1)	8.7
p_6	$d5^c$	27.9(1)	28.0
p_7	$d6^c$	16.9(1)	17.0
p_8	$d7^c$	13.6(1)	13.7
p_9	R_{bh}	120.3(3)	118.7
p_{10}	r_{CH}	111.6(5)	108.7
p_{11}	$r_{BH}(br)$	134.2(6)	127.2
p_{12}	$\angle BBB1$	108.9(2)	109.3
p_{13}	$\angle CBB1$	29.9(3)	31.9
p_{14}	$\angle BBB2$	100.2(3)	102.7
p_{15}	$\angle CBB2$	32.9(4)	33.8
p_{16}	$\angle BBH(br)$	50.7(5)	48.2
p_{17}	$\angle BBH$	127.4(12)	127.4
p_{18}	D_y	83.9(4)	81.7
p_{19}	D_z	142.6(5)	149.3
p_{20}	$\phi CBBB1$	4.1(1)	4.1
p_{21}	$\phi CBBB2$	11.7(1)	11.8
p_{22}	ring tilt	-3.8(1)	-4.0
p_{23}	H(15) tilt	-47.8(11)	-48.0
p_{24}	H(14) tilt	-60.7(12)	-60.5
p_{25}	$\phi BBBH$	64.0(12)	63.9

^a Distances in pm; angles in deg. ^b Parameters are defined fully in the Experimental Section. ^c Differences as described in text.

Table 4. Bond Distances (r_{h1}/pm) and Amplitudes of Vibration (u/pm) Obtained in the GED Refinement of **3**

u	atom pair	r_{h1}	amplitude	MP2/6-311+G*
u_1	B(1)–C(2)	169.7(5)	3.7(5)	169.5
u_2	B(1)–B(3)	182.8(3)	3.9 (tied to u_1)	179.7
u_3	B(1)–B(4)	179.6(3)	3.7 (tied to u_1)	176.4
u_6	B(1)–H(12)	120.2(3)	7.5 (tied to u_{35})	118.6
u_7	C(2)–B(3)	171.9(8)	4.0 (tied to u_1)	172.6
u_9	C(2)–B(7)	168.2(4)	3.7 (tied to u_1)	167.5
u_{11}	C(2)–H(13)	111.5(5)	6.8 (tied to u_{35})	108.8
u_{12}	B(3)–B(4)	180.6(2)	3.8 (tied to u_1)	177.4
u_{13}	B(3)–B(7)	173.0(4)	3.8 (tied to u_1)	177.3
u_{14}	B(3)–B(8)	185.2(5)	3.9 (tied to u_1)	179.1
u_{15}	B(3)–H(14)	120.2(3)	7.5 (tied to u_{35})	118.6
u_{16}	B(4)–B(5)	179.0(3)	3.6 (tied to u_1)	175.9
u_{17}	B(4)–B(8)	175.4(6)	4.0 (tied to u_1)	181.7
u_{18}	B(4)–C(9)	169.5(4)	3.7 (tied to u_1)	168.5
u_{27}	B(7)–B(8)	187.8(3)	4.1 (tied to u_1)	184.7
u_{28}	B(7)–B(11)	196.1(2)	8.4(10)	193.4
u_{30}	B(7)–H(23)	134.2(6)	9.0(10)	127.2
u_{31}	B(8)–C(9)	160.3(7)	3.7 (tied to u_1)	165.3
u_{38}	B(10)–H(24)	139.6(13)	12.3(12)	137.8

estimate the B–H and C–H bond distances as compared to the B3LYP and MP2 methods. Increasing the size of the basis set (from 6-31G* to 6-311G* at the B3LYP level and from 6-31G* to 6-311G* to 6-311+G* at the MP2 level) has little effect on the structural parameters. Indeed, there is negligible difference between the parameters calculated using the B3LYP functional method and the more computationally demanding MP2 methodology. The largest difference between these methods for compound **2** arises for the B(1)–B(4) bond, which is 1.9 pm longer at the B3LYP/6-311G* level as compared to the MP2/6-311G* value. For compound **3**, the bond distance B(7)–B(11) varies most between the methodologies employed. Without the inclusion of electron correlation, this bond is at its longest. For example, its value

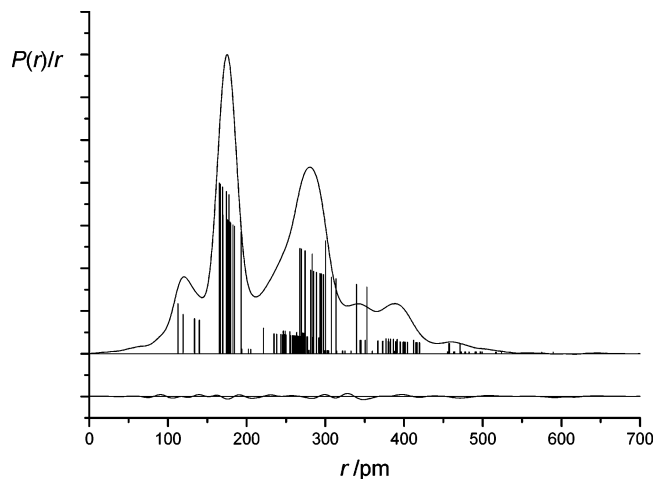


Figure 3. Experimental and difference (experimental – theoretical) radial distribution curves, $P(r)/r$ for **3**. Before Fourier inversion, the data were multiplied by $s \cdot \exp(-0.000\ 02s^2)/(Z_B - f_B)/(Z_C - f_C)$.

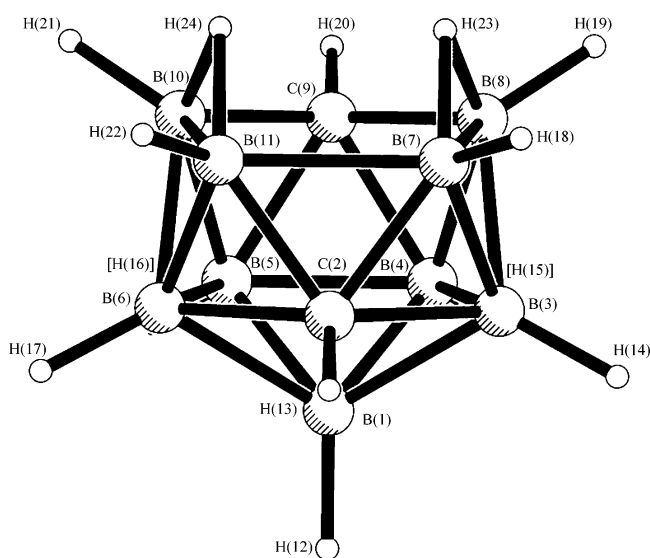


Figure 4. Molecular framework for **3**.

Table 5. Misfit (rms Deviation) Values (in Å) between GED and Optimized Geometries for **2** and **3**

method/basis set	2	3
HF/6-31G*	0.0307	0.0527
B3LYP/6-311G*	0.0305	0.0451
MP2/6-311+G*	0.0276	0.0469

at the HF/6-31G* level is 5.2 and 10.0 pm longer than at the B3LYP and MP2 levels, respectively, using equivalent basis sets.

A simple way of demonstrating how well the experimental geometries fit the optimized geometries is by a method that produces a single misfit value. This was done using the ofit command of the program *XP*,¹⁸ which gave an rms deviation between non-hydrogen atom positions. The values are shown in Table 5. The differences among the results obtained with the three methodologies are small, with the highest misfit values coming from the HF method, as would be expected.

(18) *SHELXTL-NT*, version 5.1; Bruker Analytical X-ray Instruments Inc.: Madison, WI, 1998.

Table 6. Observed (in CDCl₃) and Calculated (GIAO-B3LYP/6-311G*) ¹¹B NMR Data for **2** and **3**

boron atom	GED	observed
2,3-C ₂ B ₉ H ₁₁ (2)		
4–7	–4.5	–4.2
8, 9	–9.6	–8.5
10, 11	–7.4	–10.2
1	–16.8	–15.8
2,9-C ₂ B ₉ H ₁₃ (3)		
1	–27.2	–26.0
3, 6	–36.5	–35.3
4, 5	–7.4	–10.7
7, 11	–27.3	–25.5
8, 10	–11.3	–8.0

To assess whether the GED geometries for **2** and **3** are likely to occur also in solution, boron-11 NMR shifts were computed from these experimental structures at the GIAO-B3LYP/6-311G* level of theory. These values correspond very well to observed boron shifts for **2** and **3** in chloroform (Table 6).^{10,11} The largest difference, only 3.3 ppm, is found for B_{4,5} in **3**.

Comparison of the experimental geometries for **2** (GED) and **4** (X-ray)¹⁵ shows that the presence of methyl substituents on the carbon atoms results in lengthening of the B(1)–C(2) bond. The experimentally determined value for this bond length in **2** is 5.8 pm less than in **4**. The refined GED structure also has a B(4)–B(8) bond that is 3.6 pm shorter than those found in **4**. The opposite trend is found for the B(4)–B(10) bond: In the GED structure of **2**, this bond is 2.6 pm longer than in **4**. Comparison of the MP2/6-31G*-optimized geometries¹¹ for **2** and **4** reflects these trends, but the differences are much smaller, with a difference of 1.3 pm for the B(1)–C(2) bond. There are substantial differences in bond lengths between the experimental and optimized MP2/6-31G* geometries for **4**, with the largest difference of 4.2 pm, for the B(1)–C(2) bond. This discrepancy may be due to crystal packing forces in the experimentally determined geometry of **4**.

As there have been no derivatives of **3** reported so far, the GED geometry of **3** may only be compared with the X-ray geometry¹⁹ of a derivative of 2,7-C₂B₉H₁₃ where the cage carbon on the open face is next to C2, rather than opposite C2 as observed in **3**. Both show similar structural features on the open face, with each of the two endo hydrogens bridging a pair of boron atoms. The B–B bonds involved with the bridging hydrogens are, as expected, long, with 187.7 pm for B7–B8/B10–B11 in **3** and 185.1/185.7 pm for B8–B9/B10–B11 in the 2,7-isomer. However, even longer B–B distances are found on the open face where bridging hydrogens are not involved, with 196.1 pm for B7–B11 in **3** and 192.0 pm for B9–B10 in the 2,7-isomer. Long B–B bonds on this type of open face (i.e. CB₄ with two bridging hydrogens) are found in the related monocarbaborane anion 7-CB₁₀H₁₃[–] and its derivatives.²⁰

(19) Struchkov, Yu. T.; Antipin, M. Yu.; Stanko, V. I.; Brattsev, V. A.; Kirillova, N. I.; Knyazev, S. P. *J. Organomet. Chem.* **1977**, *141*, 133.

(20) Batsanov, A. S.; Fox, M. A.; Goeta, A. E.; Howard, J. A. K.; Hughes, A. K.; Malget, J. M. *J. Chem. Soc., Dalton Trans.* **2002**, 2624.

Table 7. GED Data Analysis Parameters for **2** and **3**

	2		3	
camera distance/mm	257.75	93.92	257.73	93.71
T_{sample}/K	440	400	465	455
T_{nozzle}/K	453	423	473	473
$\Delta s/\text{nm}^{-1}$	2	4	2	4
$s_{\text{min}}/\text{nm}^{-1}$	20	80	20	80
sw_1/nm^{-1}	40	100	40	100
sw_2/nm^{-1}	112	276	112	276
$s_{\text{max}}/\text{nm}^{-1}$	130	320	130	320
correlation param	0.4497	0.4223	0.4408	0.3817
scale factor, k^a	0.722(6)	0.612(13)	0.678(4)	0.603(10)
electron wavelength/pm	6.02	6.02	6.02	6.02

As positions of hydrogen atoms in molecular geometries determined by X-ray crystallography are not as precise as those found by GED, and they also do not represent nuclear positions, it is worth noting here that the hydrogen bridges are asymmetrical in **3**. The B–H lengths in these bridges are 134.2(6) pm for B(7)–H(23) and 139.5(12) pm for B(8)–H(23). These agree well with the values of 127.2 and 137.8 pm, respectively, calculated at the MP2/6-311+G* level of theory.

Ab initio computations were also carried out on 7,8-C₂B₉H₁₃ (**1**); geometric data at various levels of theory are listed in Supporting Information Table S9.

Experimental Section

Carboranes **1–3** were synthesized in Durham using reported procedures.^{10,11} The samples for this ED study were sublimed twice and checked for purity by NMR spectroscopy.

GED data for **2** and **3** were collected at two different camera distances using the Edinburgh apparatus.²¹ The data were recorded photographically on Kodak Electron Image films, which were converted into digital format using a PDS densitometer at the Institute of Astronomy in Cambridge with a scanning program described elsewhere.²² The weighting points for the off-diagonal weight matrices, correlation parameters, and scale factors for the two camera distances are given in Table 7, along with the electron wavelengths, which were determined from the scattering patterns of benzene vapor. The data reduction and analysis were performed using standard programs,²³ employing the scattering factors of Ross et al.²⁴ On the basis of ab initio calculations, electron diffraction refinements were carried out for **2** and **3**.

Vibrational corrections were calculated using the method of Sipachev and the program *SHRINK*,²⁵ giving refined parameters of structure type r_{h1} .

The structure of **2** was refined using 22 geometric parameters with a model of C_{2v} symmetry (Figure 2). Parameter p_1 defines the average of the bond distances B(5)–B(11), B(10)–B(11), and B(8)–B(10). The differences associated with them are defined by parameters p_2 and p_3 such that p_2 is the difference between B(5)–B(11) and B(10)–B(11) and p_3 is the difference between B(5)–B(11) and B(8)–B(10). With the origin placed at the midpoint of

the B(10)–B(11) bond, the angle between the plane B(10)B(8)B(11) and a plane perpendicular to the molecular C_2 axis is defined by p_4 . The distances between the origin and atoms B(1) and C(2) are described by parameters p_5 and p_6 . Parameter p_7 defines the angle made between atom B(1), the origin, and atom C(2), while the angle B(5)–B(11)–B(10) is defined by p_8 . Parameter p_9 describes the torsional angle B(5)–B(11)–B(10)–B(1). The mean of the bond distances B(1)–H(22), C(2)–H(17), and B(5)–H(18), and the subsequent associated differences are defined by parameters p_{10} – p_{12} . Parameter p_{11} is the difference between B(1)–H(22) and C(2)–H(17), and p_{12} is the difference between B(1)–H(22) and B(5)–H(18). The angle that H(22) makes with B(1) and B(11) is included as p_{13} , with the associated torsion with B(10) defined as p_{14} . (In practice, the last two parameters are determined by the C_{2v} symmetry of the molecule.) Angle H(17)–C(2)–B(8) and torsion H(17)–C(2)–B(8)–B(9) are defined as parameters p_{15} and p_{16} . The angle made by H(18)–B(5)–B(6) and torsion H(18)–B(5)–B(6)–B(7) are described by p_{17} and p_{18} . Angle H(13)–B(8)–C(2) and the associated torsion with B(9) are defined by p_{19} and p_{20} , respectively. The final two parameters, p_{21} and p_{22} , define the angle H(14)–B(11)–B(10) and torsion H(14)–B(11)–B(10)–B(1), respectively.

The structure of **3** was refined with a model of C_s symmetry using 25 geometric parameters (Figure 4). Parameter p_1 defines the average of the bond distances B(7)–B(11), B(4)–B(5), B(5)–B(6), C(2)–B(6), B(7)–B(8), B(8)–C(9), B(1)–B(5), and B(1)–B(6). The differences between B(7)–B(11) and each of these bond distances are defined by parameters p_2 – p_8 , respectively. Parameter p_9 describes the terminal B–H bond distances, while the C–H and bridging B–H distances are defined by p_{10} and p_{11} . The angles B(4)–B(5)–B(6), C(2)–B(3)–B(6), B(8)–B(7)–B(11), and C(9)–B(10)–B(8) are defined as p_{12} – p_{15} , respectively. Parameter p_{16} defines the angle B(7)–H(23)–B(8). The angle B(5)–B(1)–H(12) is defined by p_{17} . Parameters p_{18} and p_{19} describe the displacements in the y (perpendicular to the plane of the paper in Figure 4) direction and z (vertical) direction when moving the origin from the midpoint of B(3)–B(6) to the midpoint of B(7)–B(11). The torsional angles C(2)–B(3)–B(6)–B(5) and C(9)–B(8)–B(10)–B(11), which describe the movement of each carbon out of the plane of its respective ring, are defined by p_{20} and p_{21} . In addition to the displacement between the rings, on the basis of ab initio calculations, there is a significant tilt of the upper ring such that atoms B(8), C(9), and B(10) move away from the lower ring. This tilt is defined by p_{22} . If the origin is moved to the center of the boron cage, the angles origin–B(5)–H(16) and origin–B(4)–H(15) are defined by p_{23} , while the angles origin–B(3)–H(14) and origin–B(6)–H(17) are defined by p_{24} . Parameter p_{25} describes the torsion B(4)–B(5)–B(1)–H(12).

Computational Section

NMR chemical shifts were calculated using the *Gaussian98*²⁶ package. The non-hydrogen atoms of experimental and calculated

- (21) Huntley, C. M.; Laurenson, G. S.; Rankin, D. W. H. *J. Chem. Soc., Dalton Trans.* **1980**, 954.
 (22) Lewis, J. R.; Brain, P. T.; Rankin, D. W. H. *Spectrum* **1997**, 15, 7.
 (23) Hinchley, S. L.; Robertson, H. E.; Borisenko, K. B.; Turner, A. R.; Johnston, B. F.; Rankin, D. W. H.; Ahmadian, M.; Jones, J. N.; Cowley, A. H. Manuscript in preparation.
 (24) Ross, A. W.; Fink, M.; Hilderbrandt, R. *International Tables for Crystallography*; Wilson, A. J. C., Ed.; Kluwer Academic Publishers: Dordrecht, The Netherlands, 1992; Vol. C, p 245.
 (25) Sipachev, V. A. *THEOCHEM* **1985**, 121, 143.

- (26) Frisch, M. J.; Trucks, G. W.; Schlegel, H. B.; Scuseria, G. E.; Robb, M. A.; Cheeseman, J. R.; Zakrzewski, V. G.; Montgomery, J. A., Jr.; Stratmann, R. E.; Burant, J. C.; Dapprich, S.; Millam, J. M.; Daniels, A. D.; Kudin, K. N.; Strain, M. C.; Farkas, O.; Tomasi, J.; Barone, V.; Cossi, M.; Cammi, R.; Mennucci, B.; Pomelli, C.; Adamo, C.; Clifford, S.; Ochterski, J.; Petersson, G. A.; Ayala, P. Y.; Cui, Q.; Morokuma, K.; Malick, D. K.; Rabuck, A. D.; Raghavachari, K.; Foresman, J. B.; Cioslowski, J.; Ortiz, J. V.; Stefanov, B. B.; Liu, G.; Liashenko, A.; Piskorz, P.; Komaromi, I.; Gomperts, R.; Martin, R. L.; Fox, D. J.; Keith, T.; Al-Laham, M. A.; Peng, C. Y.; Nanayakkara, A.; Gonzalez, C.; Challacombe, M.; Gill, P. M. W.; Johnson, B. G.; Chen, W.; Wong, M. W.; Andres, J. L.; Head-Gordon, M.; Replogle, E. S.; Pople, J. A. *Gaussian 98*, revision A.7; Gaussian, Inc.: Pittsburgh, PA, 1998.

geometries were compared using the *ofit* command of *XP*,¹⁸ which produces an rms deviation or misfit value.

Geometry optimizations for compounds **1**, **2**, and **3** were performed using HF (3-21G* and 6-31G* basis sets), density functional theory (DFT) (6-31G* and 6-311G* basis sets using the B3LYP functional method), and MP2 (6-31G*, 6-311G*, and 6-311+G* basis sets) methods. The resultant geometrical parameters are given in Supporting Information Tables S9, S1, and S5 for compounds **1**, **2**, and **3**, respectively.

Frequency calculations allowed the nature of stationary points to be investigated, confirming the structures as local minima, transition states, or higher-order stationary points on the potential-energy surfaces. The starting parameters for the r_{hl} refinements were taken from the theoretical geometries at the HF/6-31G* level.

Theoretical (HF/6-31G*) Cartesian force fields were obtained and converted into force fields described by sets of symmetry coordinates using the *SHRINK* program.²⁵ All geometric parameters were then refined.

Acknowledgment. We thank the Engineering and Physical Sciences Research Council for support (Grant GR/R17768).

Supporting Information Available: Data tables (DFT calculations, bond lengths and calculations, correlation matrices), and molecular scattering intensity graphs. This material is available free of charge via the Internet at <http://pubs.acs.org>.

IC0494509